

## Pion-induced nucleon knockout from polarized nuclei

N. S. Chant and P. G. Roos

*Department of Physics and Astronomy, University of Maryland, College Park, Maryland 20742*

(Received 22 April 1988)

Distorted wave impulse approximation predictions are made for quasifree ( $\pi, \pi N$ ) nucleon knockout reactions on polarized nuclear targets. The case of  $J_A = \frac{1}{2}$  targets is considered in detail with particular reference to  $^{13}\text{C}$ . It is shown, for this case, that three terms, having somewhat different physical origins, contribute to the spin-up/spin-down asymmetry.

### I. INTRODUCTION

Plans and developments are underway at a number of laboratories to permit studies of pion-induced nuclear reactions using polarized target nuclei. Recently, effects in pion charge exchange and in  $(\pi^+, \eta)$  reactions have been discussed.<sup>1</sup> Here we consider quasifree nucleon knockout reactions of the type  $(\pi, \pi N)$ . Such experiments have become technically feasible<sup>2,3</sup> and may perhaps be considered a potentially rich source of information, not only on the spin dependence of the pion-nucleon interaction within the nuclear medium, but also of details of the reaction dynamics. We attempt to illustrate the several distinct features which contribute to the overall target spin projection dependence of the reaction cross section and thus provide guidance for future experimental studies.

Our discussion is in terms of a conventional factorized distorted wave impulse approximation (DWIA) treatment of the  $(\pi, \pi N)$  reaction. This should be a reasonable guide in the case of  $(\pi^+, \pi^+ p)$  and  $(\pi^-, \pi^- n)$  reactions. Factorized DWIA calculations provide a very good description of  $^{12}\text{C}(\pi^+, \pi^+ p)^{11}\text{B}$  data,<sup>4</sup> and estimates of the  $\Delta$ - $N$  knockout term<sup>2,5</sup> suggest that it is less than 10% of the nucleon knockout cross section in this  $T = \frac{3}{2}$   $\pi$ - $N$  channel. However, for the  $(\pi^+, \pi^+ n)$  and  $(\pi^-, \pi^- p)$  reactions the  $\Delta$ - $N$  terms introduce large effects, so that our calculations are inappropriate for these cases.

For simplicity in the present paper, we consider only coplanar geometries and the case of  $J = \frac{1}{2}$  targets. Several important features of the target polarization dependence will be illustrated. In addition, predictions for the  $(\pi^-, \pi^- n)$  reaction on a polarized  $^{13}\text{C}$  target will be shown for several final states in  $^{12}\text{C}$ .

### II. DWIA FORMALISM

In previous papers we discussed aspects of distorted wave effects in pion-induced knockout reactions<sup>6,7</sup> and have shown comparisons with experimental data for

$^{12}\text{C}(\pi^+, \pi^+ p)^{11}\text{B}$  reactions.<sup>4</sup> Here we take into account the possibility of polarized target nuclei. In view of the emphasis on the spin-dependent aspects of the process, we have also included the possibility of spin-dependent distortions for the emitted nucleon. Our approach closely follows our treatment of  $(p, 2p)$  reactions.<sup>8</sup> In particular, we again employ a direct three-dimensional integration of the DWIA amplitude in order to avoid rather complicated and time-consuming computation of many vector coupling coefficients along with a large number of radial integrals.

Let us consider a reaction  $A(a, cd)B$  where  $A = B + b$ . Particles  $a$  and  $c$  are spinless while  $b$  and  $d$  have spin  $\frac{1}{2}$ . For such a reaction the amplitude for a transition from an initial target angular momentum and projection  $J_A, M_A$  to a residual nucleus state  $J_B, M_B$  may be written

$$T_{BA} = \sqrt{A} \sum_{\lambda \sigma m \tau}^{lsjt} \mathcal{J}_{AB}(nlsjt)(J_B M_B jm | J_A M_A) \times (T_B N_B t \tau | T_A N_A)(l \lambda s \sigma | jm) \times \langle \phi_c \phi_d | t | \phi_a \phi_{l\lambda}(\mathbf{r}) X_{\sigma\tau}^{\text{st}} \rangle. \quad (1)$$

The quantum numbers  $j, m$  represent the total angular momentum and angular momentum projection of the struck particle  $b$ . This is made up of orbital angular momentum  $l, \lambda$  and spin  $s = \frac{1}{2}, \sigma$ . The corresponding isospin quantum numbers for  $b$  are  $t, \tau$  and for particle  $i$  are  $T_i, N_i$ . The quantities  $(j_1 m_1 j_2 m_2 | j_3 m_3)$  are vector coupling coefficients. The amplitude  $\mathcal{J}_{AB}$  is related to the conventional single nucleon spectroscopic factor through  $s = A \mathcal{J}_{AB}^2$ , where  $A$  is the number of target nucleons. The quantity  $\langle | t | \rangle$  is a transition amplitude in which the  $\phi_i$  are wave functions for the incident and emitted particles, while  $\phi_{l\lambda}$  is the spatial wave function and  $X_{\sigma\tau}^{\text{st}}$  the spin/isospin wave function for the struck particle  $b$ .

Making the usual impulse approximation we can write the cross section for angular momentum projection  $M'_A$  for the target:

$$\sigma_{BA}(M'_A) = \frac{2\pi}{\hbar v} \omega_B \sqrt{A} \sum_{M_B \rho'_d} \left| \sum_{\lambda \sigma m \tau M_A \sigma'_d} \mathcal{J}_{AB}(nlsjt)(J_B M_B jm | J_A M_A) D_{M'_A M_A}^J(R_{ap})(T_B N_B t \tau | T_A N_A)(l \lambda s \sigma | jm) \times T_{\sigma'_d \rho'_d}^{l\lambda} \langle \sigma'_d, \mathbf{k}' | t | \sigma; \mathbf{k} \rangle \right|^2, \quad (2)$$

where  $v$  is the projectile velocity,  $\omega_B$  the energy density of final states, and  $\langle \sigma_d''; \mathbf{k}' | t | \sigma; \mathbf{k} \rangle$  the two-body transition amplitude for the  $b(a,c)d$  reaction. For the DWIA transition amplitude  $T$  we have

$$T_{\sigma_d'' \rho_d''}^{l\lambda} = \int \chi_c^{(-)*} \chi_{\sigma_d'' \rho_d''}^{(-)*} \phi_{l\lambda} \chi_a^{(+)} d^3r, \quad (3)$$

where the  $\chi$  are distorted waves for the incident and emitted particles. Since the spin of particle  $d$  is  $\frac{1}{2}$ , the corresponding distorted wave is a matrix in spin space in terms of the projection quantum numbers  $\sigma_d'', \rho_d''$ . As is customary in this type of calculation, it is convenient to choose the axis of quantization along the incident particle direction. As a result, the rotation operator  $D_{M_A M_A'}^{J_A}$ , is included so that other orientations of the target polarization may be considered.<sup>9</sup> In all the following calculations, it is assumed that the target is polarized along the normal to the scattering plane.

As discussed earlier,<sup>8</sup> as a practical matter, it is convenient to introduce different quantization axes for particles  $a$ ,  $c$ , and  $d$ . Thus in our computations additional rotational matrices enter to permit correct evaluation of the amplitudes.

It is interesting to note that, in contrast to the case of an unpolarized target, different values of  $j$  enter coherent-

ly in the cross section. Examples of this situation will be considered.

### III. QUALITATIVE FEATURES OF THE TARGET SPIN PROJECTION DEPENDENCE

The expressions outlined above have been coded for the computer in order to permit predictions for the target spin orientation dependence of the cross section. Results will be shown in Sec. IV. However, in order to plan future experimental studies effectively, it is important to understand the physical origin of the major spin-dependent contributions to the reaction.

As an example, we restrict the reaction to a coplanar geometry in which the momenta of particles  $a$ ,  $c$ , and  $d$  lie in a common plane. In addition, we will assume that the target nucleus  $A$  is polarized along a direction normal to the scattering plane. Finally, we will ignore possible spin dependence of the emitted nucleon distorted wave so that  $T$  becomes diagonal in  $\sigma_d'', \rho_d''$ . With these restrictions it becomes advantageous to choose the axis of quantization normal to the scattering plane so that the rotation matrix  $D_{M_A M_A'}^{J_A}$ , is a unit matrix and Eqs. (2) and (3) may be rewritten

$$\sigma_{BA}(M_A) = \frac{2\pi}{\hbar v} \omega_B \sqrt{A} \sum_{M_B \sigma_d''} \left| \sum_{\lambda \sigma m \tau}^{lsjt} \mathcal{J}_{AB}(nlsjt) (J_B M_B j m | J_A M_A) (T_B N_B t \tau | T_A N_A) (l\lambda s \sigma | j m) T^{l\lambda} \langle \sigma_d''; \mathbf{k}' | \sigma; \mathbf{k} \rangle \right|^2, \quad (4)$$

where

$$T^{l\lambda} = \int \chi_c^{(-)*} \chi_d^{(-)*} u(r) Y_{l\lambda}(\hat{r}) \chi_a^{(+)} d^3r \quad (5)$$

and we have written the bound nucleon wave function explicitly in terms of a radial function  $u(r)$ , and a spherical harmonic,  $Y_{l\lambda}(\hat{r})$ .

Symmetry arguments lead to valuable simplification of these expressions, specifically for the spherical harmonic,<sup>9</sup>

$$Y_{l\lambda}(\theta, \phi) = (-)^{l+\lambda} Y_{l\lambda}(\pi - \theta, \phi) \quad (6)$$

and for a coplanar geometry, the remaining terms in the integrand are mirror symmetric with respect to the scattering plane. Thus, with our present choice of  $z$  axis, these terms are identical for polar angles  $\theta$  and  $\pi - \theta$ . Combining this feature with the symmetry relationship (6) leads to the result that the integral is nonzero only if  $l + \lambda$  is even. As a result, the summation over  $\lambda$  and  $\sigma$  becomes incoherent since, for each value of  $m$ ,  $\lambda = m \pm \frac{1}{2}$  and terms of the form  $T^{l\lambda} T^{l\lambda'*}$  must vanish if  $\lambda \neq \lambda'$ . Thus, we write

$$\sigma_{BA}(M_A) \sim \sum_{M_B \sigma_d''} (J_B M_B j m | J_A M_A)^2 (l\lambda s \sigma | j m)^2 | T^{l\lambda} |^2 \langle \sigma_d''; \mathbf{k}' | t | \sigma; \mathbf{k} \rangle^2, \quad (7)$$

where spin-independent factors have been omitted and we consider only a single value of  $j$ .

Since initial studies are likely to employ light targets, we will consider only knockout of nucleons from the  $1s$  and  $1p$  shells. In addition, we will restrict discussion to  $J_A = \frac{1}{2}$  targets such as  $^{13}\text{C}$ .

For the possible transitions resulting from  $1p$  nucleon removal the DWIA result (7) simplifies to the following

expression for  $M_A = \pm \frac{1}{2}$ :

$$\sigma(M_A = \pm \frac{1}{2}) = \sigma_0 (1 \pm P_s A \pm P_0 P + \alpha P A), \quad (8)$$

where  $\sigma_0$  combines all spin-independent factors,  $A$  is the polarization analyzing power in  $\pi$ -nucleon scattering, and  $P$  is defined as

$$P = \frac{|T^{11}|^2 - |T^{1-1}|^2}{|T^{11}|^2 + |T^{1-1}|^2}, \quad (9)$$

with  $T^{10}$  equal to zero. Clearly  $P$  is to be regarded as an effective polarization in orbital angular momentum. It is essentially the quantity termed "Newns polarization" in Ref. 1. It is well known from the early studies of stripping and pickup reactions<sup>10</sup> as well as nucleon knockout reactions on unpolarized targets.<sup>11,12</sup>

This effect can be understood by dividing the nucleus by a plane containing the  $z$  axis and the recoil momentum of the residual nucleus  $\mathbf{q}$ . Since the orbital angular momentum transfer can be written  $\mathbf{l} = \mathbf{r} \times \mathbf{q}$  it follows that any distortion effect which leads to unequal contributions from the two hemispheres will lead to an effective polarization in  $\mathbf{l}$ . An example of such an effect is a difference in mean free path of the two emitted particles which will lead to localization of the reaction on one side of the nucleus. In the plane wave limit for  $p$ -shell nucleon knockout  $P=0$ . (It is identically zero for  $s$ -shell nucleon knockout.)

The coefficients  $\alpha$ ,  $P_0$ , and  $P_s$  are listed in Table I. We see that, even if  $P=0$ , there is a spin-dependent term  $P_s A$ . We can obtain the values of  $P_s$  listed by computing the probabilities  $C_{\pm}$  of obtaining spin-up or spin-down nucleons in the target wave function (projected onto the various residual and transferred angular momenta) but including only  $\lambda = \pm 1$  substates. Specifically,

$$C_{\pm} = \sum_{\substack{m M_B \\ \lambda = \pm 1}} (J_B M_B j m | J_A M_A)^2 (1 \lambda \frac{1}{2} \pm \frac{1}{2} | j m)^2. \quad (10)$$

This is equivalent to evaluating the DWIA expression in a plane wave (or attenuated plane wave) approximation in which the quantities  $|T^{11}|^2$  and  $|T^{1-1}|^2$  are equal. We refer to  $P_s$  as the "spin polarization." As an example, we see that, for the  $p_{1/2}$  transition to a  $0^+$  final state, the nucleon spin is exactly antiparallel to the target spin.

The coefficient  $P_0$  we refer to as the "orbital polarization." We can obtain the values listed by computing the differing probabilities  $D_{\pm}$  of obtaining  $\lambda = \pm 1$  in the projected target wave function for the various transitions. Specifically,

$$D_{\pm} = \sum_{m M_B \sigma} (J_B M_B j m | J_A M_A)^2 (1 \pm 1 \frac{1}{2} \sigma | j m)^2. \quad (11)$$

Whether a given term can contribute to the cross section is determined by the values of  $|T^{1\pm 1}|^2$ , and hence the

corresponding polarization analyzing power is simply  $P$ , and a term  $P_0 P$  remains even if  $A=0$ . Finally, the coefficient  $\alpha$  converts the effective polarization in  $\mathbf{l}$  to an effective polarization in the nucleon spin. This leads to a term  $\alpha P A$  which differs only between  $p_{1/2}$  and  $p_{3/2}$  transitions and remains even after averaging over  $M_A$ . This term is well known from analyses of  $(p, 2p)$  reactions induced by unpolarized protons in which the reaction cross section involves a factor  $(1 + \mathbf{A} \cdot \mathbf{P}_{\text{eff}})$ , where  $P_{\text{eff}} = \alpha P$ .

For  $s_{1/2}$  nucleon knockout, the effective polarization is zero and thus for transitions to  $0^-$  or  $1^-$  final states Eq. (8) simplifies to

$$\sigma(M_A = \pm \frac{1}{2}) = \sigma_0(1 \pm A), \quad (12)$$

where we see that only the term  $P_s A$  is present with  $P_s = 1$ .

#### IV. QUANTITATIVE FEATURES OF THE TARGET SPIN PROJECTION DEPENDENCE

We next present a series of factorized DWIA calculations of the  $^{13}\text{C}(\pi^-, \pi^- n)^{12}\text{C}$  reaction in order to demonstrate various effects, as well as to provide information for experimental planning. The chosen incident  $\pi^-$  energy is 165 MeV, an energy at which we expect effective polarizations to be large due to strong distortion (particularly absorption) effects and for which good beam intensities are available at the meson factories.

Calculations of the energy sharing cross sections will be presented for three quasifree angle pairs—angle pairs for which it is kinematically allowed to leave the ground state of the residual nucleus at rest. These angle pairs are listed in Table II along with the corresponding two-body  $\pi^- n$  center-of-mass angles, differential cross sections, and analyzing powers at approximately  $T_{\pi} = 148$  MeV (which roughly matches the average energy of the  $\pi^- n$  final state in the  $^{13}\text{C}(\pi^-, \pi^- n)$  reaction). It should be noted that our studies cover a range from smaller ( $\pi^- n$ ) cross sections and large analyzing powers to large cross sections and very small analyzing powers. This allows us to better separate the effects from the various terms present in Eq. (8).

In all calculations we have used a Kisslinger-type  $\pi$ -nucleus optical model potential to calculate the incoming and outgoing pion distorted waves. The parameters for the incoming pion were taken from the resonance energy  $\pi$ -nucleus elastic scattering analysis of Cottingham and Holtkamp.<sup>13</sup> Those for the lower energy outgoing pion were taken from the energy-dependent analysis of  $\pi$ - $^{12}\text{C}$

TABLE I. Values of the effective polarization parameters for  $1s$  and  $1p$  transitions in  $^{13}\text{C}$ .

Transitions	$P_s$	$P_0$	$\alpha$
$P_{1/2} \rightarrow 0^+$	-1	1	-1
$\rightarrow 1^+$	$\frac{1}{3}$	$-\frac{1}{3}$	-1
$P_{3/2} \rightarrow 1^+$	$\frac{2}{3}$	$\frac{5}{6}$	$\frac{1}{2}$
$\rightarrow 2^+$	$-\frac{2}{5}$	$-\frac{1}{2}$	$\frac{1}{2}$
$S_{1/2} \rightarrow 0^-$	1	0	0
$\rightarrow 1^-$	1	0	0

TABLE II. Laboratory angle pairs and two-body ( $\pi$ - $N$ ) on-shell data at  $T_{\pi} = 148$  MeV for the  $^{13}\text{C}(\pi^-, \pi^- n)^{12}\text{C}$  DWIA calculations presented in this paper.

$\theta_{\pi}$	$\theta_p$	$\theta_{\pi^- n}^{\text{c.m.}}$	$\frac{d\sigma}{d\Omega}$	(mb/sr)	$A_{\pi^- n}$
60	-49.5	74.2°		8.5	0.44
100	-30.5	115.2°		12.2	0.15
140	-14.5	149.4°		23.6	0.02

elastic scattering by Amann *et al.*<sup>14</sup> The optical potentials for the outgoing proton were obtained from the global analysis of medium energy proton elastic scattering by Nadasen *et al.*<sup>15</sup> Finally, the nucleon bound state parameters were obtained from the work of Elton and Swift.<sup>16</sup>

In the following subsection we will first present a series of calculations illustrating various aspects of the reaction. We will then present specific predictions for  $^{13}\text{C}(\pi^-, \pi^-n)^{12}\text{C}$  using the Cohen-Kurath<sup>17</sup> shell model wave functions.

### A. Polarization effects in DWIA calculations

To illustrate the role of the terms which arise in Eq. (8), we have carried out a series of calculations for five pure transitions:  $1s_{1/2}$  knockout ( $\frac{1}{2}^- \rightarrow 0^-$ ),  $1p_{1/2}$  knockout ( $\frac{1}{2}^- \rightarrow 0^+, 1^+$ ), and  $1p_{3/2}$  knockout ( $\frac{1}{2}^- \rightarrow 1^+, 2^+$ ). To prevent  $Q$ -value differences from obscuring the polarization effects of interest, we have taken all final states (including the  $0^-$  state) to be degenerate with a separation energy of 12.5 MeV (approximately the average separation energy for  $^{13}\text{C} \rightarrow ^{12}\text{C}$ ). Furthermore, to emphasize the differences between the  $p_{1/2}$  and  $p_{3/2}$  transitions which arise from polarization effects we have set the bound state spin-orbit potential equal to zero; i.e., the radial wave functions for the  $p_{1/2}$  and  $p_{3/2}$  bound states are identical. Finally, most of the calculations are carried out with no spin-orbit potential for the knocked out nucleon. As a result Eq. (8) should correctly describe the various effects. Changes due to the spin-orbit potential will be examined at the end of this subsection.

#### 1. Effective polarization

Firstly, we have calculated the effective polarizations  $P_{\text{eff}} = \alpha P$  defined in Eqs. (8) and (9) for  $p_{1/2}$  and  $p_{3/2}$  knockout arising from the differing distortions of the two

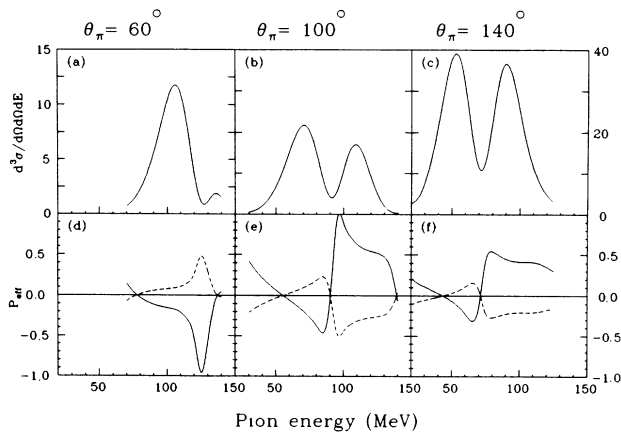


FIG. 1. Effective polarizations ( $P_{\text{eff}} = \alpha P$ ) for  $^{13}\text{C}(\pi^-, \pi^-n)$  at 165 MeV. The top graphs show the  $p_{1/2}$  knockout energy sharing cross sections (arbitrary units) for the three angle pairs of Table II,  $\theta_\pi = 60^\circ$  (a),  $\theta_\pi = 100^\circ$  (b), and  $\theta_\pi = 140^\circ$  (c). The lower graphs [(d)–(f)] show the effective polarizations  $P_{\text{eff}}$  for  $p_{1/2}$  (—) and  $p_{3/2}$  (---) knockout at the same angle pairs.

emergent particles. These are shown in Fig. 1 for the energy sharing distributions for the three angle pairs in Table II. For orientation, the top graphs [(a)–(c)] show the  $p_{1/2}$  knockout differential cross section at these angle pairs. In spite of distortion effects, each cross section exhibits a pronounced minimum near zero recoil momentum due to the  $l = 1$  wave function. The asymmetries in the peaks arise primarily from the energy dependence of the two-body  $\pi^-n$  cross section.

The effective polarizations are presented in the lower graphs [(d)–(f)]. Several observations can be made. Firstly, the effective polarization is generally quite large at all angle pairs, even at maxima in the cross sections. Therefore, we expect the terms containing  $P$  in Eq. (8) to be important for all  $p$ -shell knockout analyzing powers, although it will be least important at forward pion angles. Secondly, we note that

$$P_{\text{eff}}(p_{1/2}) = -2P_{\text{eff}}(p_{3/2}),$$

as implied by the values of  $\alpha$ , since we have taken the orbits to be degenerate and the spin-orbit potential to be zero. This simply arises from the fact that, if there is no spin-orbit splitting, one cannot distinguish between  $p_{3/2}$  and  $p_{1/2}$  and the sum of the analyzing powers weighted by  $(2j + 1)$  must be zero. This has already been discussed for  $(p, 2p)$  reactions.<sup>18</sup> Even when spin-orbit splitting is included, this relationship is approximately true and can be used experimentally to isolate these effective polarization effects.

#### 2. Analyzing powers for transitions to specific states

Next we show calculations of cross sections and analyzing power for the knockout of  $s_{1/2}$ ,  $p_{1/2}$ , and  $p_{3/2}$  neutrons from a polarized  $^{13}\text{C}$  target ( $\frac{1}{2}^-$ ). The analyzing power  $A_{\text{TGT}}$  is defined through the expression

$$\sigma = \sigma_0(1 + \mathbf{A}_{\text{TGT}} \cdot \mathbf{P}_{\text{TGT}}), \quad (13)$$

where  $\mathbf{P}_{\text{TGT}}$  is the polarization of the  $^{13}\text{C}$  target. Thus using Eq. (8) we obtain

$$A_{\text{TGT}} = \frac{P_s A + P_0 P}{1 + \alpha P A} \quad (14)$$

for the  $1p$  transitions. No  $p_{1/2}, p_{3/2}$  admixtures for the  $1^+$  transitions are considered at this point. Calculations are presented in Figs. 2 and 3 for two pion angles, the forward angle of  $60^\circ$  (Fig. 2) at which the effective polarization  $P$  is relatively small (except near zero recoil momentum) and the  $\pi^-n$  analyzing power  $A$  is large (0.44), and the largest angle  $140^\circ$  (Fig. 3) at which  $P$  is large and  $A$  is essentially zero ( $< 0.02$ ).

The left-most graphs [(a) and (d)] in both figures show the cross sections and analyzing powers for  $1s_{1/2}$  knockout to a  $0^-$  final state ( $\frac{1}{2}^- \rightarrow 0^-$  transition). As expected the cross section peaks near zero recoil momentum. As indicated in Eq. (10), the analyzing power is simply equal to the  $\pi^-n$  two-body analyzing power, the small changes resulting from the variations in the  $\pi^-n$   $t$  matrix due to changes in the  $\pi^-n$  c.m. energy in the final state.

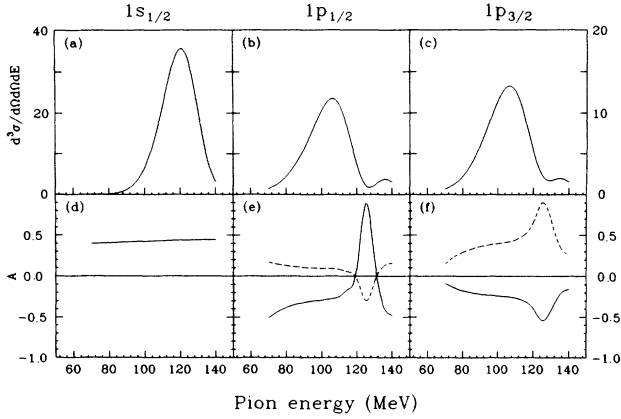


FIG. 2. Energy sharing cross sections and analyzing powers for  $^{13}\text{C}(\pi^-, \pi^- n)^{12}\text{C} (J^\pi)$  at 165 MeV and  $\theta_\pi = 60^\circ / \theta_n = -49.5^\circ$ . The cross sections ( $\mu\text{b}/\text{sr}^2 \text{MeV}$ ) are for (a)  $1s_{1/2}$  (left scale), (b)  $1p_{1/2}$  (right scale), and (c)  $1p_{3/2}$  (right scale) knockout assuming a spectroscopic amplitude of unity. The analyzing powers are (d)  $1s_{1/2}$  knockout,  $\frac{1}{2}^- \rightarrow 0^-$ ; (e)  $1p_{1/2}$  knockout, solid line  $\frac{1}{2}^- \rightarrow 0^+$ , dashed line  $\frac{1}{2}^- \rightarrow 1^+$ ; (f)  $1p_{3/2}$  knockout, solid line  $\frac{1}{2}^- \rightarrow 2^+$ , dashed line  $\frac{1}{2}^- \rightarrow 1^+$ .

The center [(b) and (e)] and right [(c) and (f)] graphs of Figs. 2 and 3 correspond to  $p_{1/2}$  and  $p_{3/2}$  knockout, respectively. The unpolarized cross sections are nearly the same for all  $p$ -shell knockout states, since we took a spectroscopic factor of 1 for each case. There are, of course, small effects due to the effective polarizations of the target nucleon.

The analyzing powers vary extensively and reflect the various terms in Eq. (8). For example, at forward angles ( $60^\circ$  in Fig. 2)  $A$  is rather large and positive ( $A \approx 0.44$ )

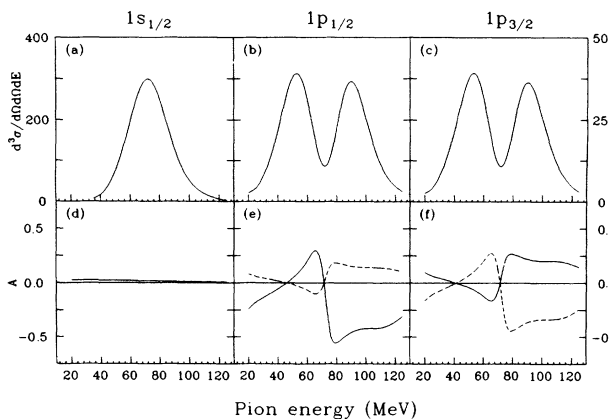


FIG. 3. Energy sharing cross sections and analyzing powers for  $^{13}\text{C}(\pi^-, \pi^- n)^{12}\text{C} (J^\pi)$  at 165 MeV and  $\theta_\pi = 140^\circ / \theta_n = -14.5^\circ$ . The cross sections ( $\mu\text{b}/\text{sr}^2 \text{MeV}$ ) are for (a)  $1s_{1/2}$  (left scale), (b)  $1p_{1/2}$  (right scale), and (c)  $1p_{3/2}$  (right scale) knockout assuming a spectroscopic amplitude of unity. The analyzing power are (d)  $1s_{1/2}$  knockout,  $\frac{1}{2}^- \rightarrow 0^-$ ; (e)  $1p_{1/2}$  knockout, solid line  $\frac{1}{2}^- \rightarrow 0^+$ , dashed line  $\frac{1}{2}^- \rightarrow 1^+$  (f)  $1p_{3/2}$  knockout, solid line  $\frac{1}{2}^- \rightarrow 2^+$ , dashed line  $\frac{1}{2}^- \rightarrow 1^+$ .

while  $P_{\text{eff}} \approx 0.17$  at the peak of the cross section. As a result the first term in Eq. (14) tends to dominate, as we see for  $T_\pi = 105$  MeV outgoing pion energy, where the analyzing powers are roughly proportional to the values of  $P_s$  listed in Table I.

In contrast, at large angles,  $\theta_\pi = 140^\circ$ , the two-body analyzing power is essentially zero. Therefore, the three-body analyzing powers in Fig. 3 are simply  $P_0 P = P_0 P_{\text{eff}} / \alpha$  (where the effective polarizations,  $P_{\text{eff}}$ , are presented in Fig. 1).

It is clear from these calculations that experiments oriented toward studies of the effective  $\pi$ - $N$  interaction in the nuclear medium will have to concentrate on the forward pion angles. On the other hand, measurements at large angles would be appropriate for general reaction dynamics studies testing distorted wave treatments of the reaction.

### 3. $p_{1/2}, p_{3/2}$ admixtures for $\frac{1}{2}^-$ to $1^+$ transitions

As indicated in Eq. (2), in contrast to the case of an unpolarized target, different values of angular momentum  $j$  of the struck nucleon contribute coherently. For  $^{13}\text{C}$  only the  $\frac{1}{2}^-$  to  $1^+$  transitions allow admixtures of  $p_{1/2}$  and  $p_{3/2}$  knockout. In the Cohen-Kurath wave functions the  $p_{3/2}$  term is dominant. Nevertheless, it is of interest to examine the effects of the coherence by varying the  $p_{1/2}$  and  $p_{3/2}$  admixture.

In Fig. 4 we present results for  $p_{1/2}$  and  $p_{3/2}$  spectroscopic amplitudes ( $a_{1/2}, a_{3/2}$ ) of (1.0,0.0), (0.0,1.0), (0.866,  $\pm 0.5$ ), and (0.5,  $\pm 0.866$ ). Although there is some variation in cross section ( $\lesssim 25\%$ ), the major and easily identifiable differences are present in the target analyzing power. We have therefore presented in Fig. 4 only the analyzing power calculations at the three angle pairs.

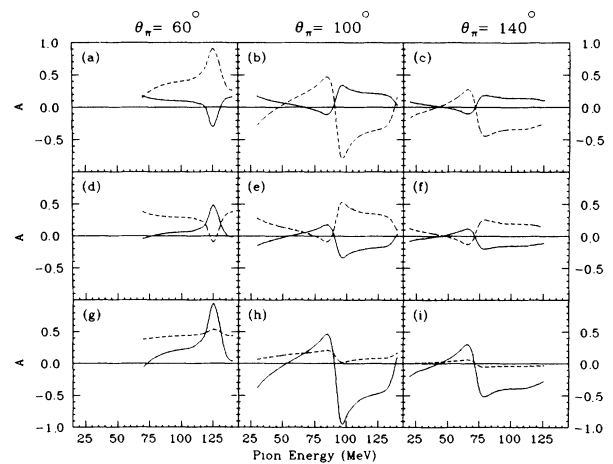


FIG. 4. Analyzing powers for  $\frac{1}{2}^-$  to  $1^+$  transitions for various  $p_{1/2}$  and  $p_{3/2}$  admixtures at three angle pairs  $60^\circ$  [(a), (d), and (g)],  $100^\circ$  [(b), (e), and (h)], and  $140^\circ$  [(c), (f), and (i)]. Labeling the amplitudes by  $(a_{p_{1/2}}, a_{p_{3/2}})$  the admixtures are (a)–(c) (1.0,0.0) solid line, (0.0,1.0) dashed line; (d)–(f) (0.866,0.5) solid line, (0.866,−0.5) dashed line; (g)–(i) (0.5,0.866) solid line, (0.5,−0.866) dashed line.

Examination of the various curves shows strong sensitivity to the degree of admixture. It would also appear that the  $p_{3/2}$  term carries somewhat more weight than the  $p_{1/2}$  term. Other than these few general comments it is difficult to make more quantitative statements with respect to the relationship between the analyzing power and degree of admixture. Data for  $1^+$  transitions will have to be compared to the coherent calculations. Clearly, however, in the case of significant admixtures of different  $j$  values, it is likely that the relative sign of the amplitudes can be determined unambiguously.

#### 4. Spin-orbit effects due to emergent nucleon

In all of the previous calculations the spin-orbit potential in the optical model potential for the ejected nucleon was set to zero. We now examine the effects of the nucleon spin-orbit potential on the  $(\pi^-, \pi^- n)$  reaction.

In Fig. 5 we present calculations at all three angle pairs for three representative transitions,  $1s_{1/2}$  knockout ( $\frac{1}{2}^- \rightarrow 0^-$ ),  $1p_{1/2}$  knockout ( $\frac{1}{2}^- \rightarrow 0^+$ ), and  $1p_{3/2}$  knockout ( $\frac{1}{2}^- \rightarrow 2^+$ ). Generally the spin-orbit effects are sufficiently small so that they do not destroy the various features discussed in Sec. IV A 2. We do observe a large change in the  $s_{1/2}$  analyzing powers at low energy, but this is probably of little interest experimentally since in this region the cross section is extremely small and very sensitive to small changes in the distorted waves.

Calculations of the analyzing powers for  $p$ -shell transitions are presented in the lower graphs of Fig. 5. We see that the spin-orbit potential has very little effect on the  $p_{3/2}$  knockout analyzing power. However, there are

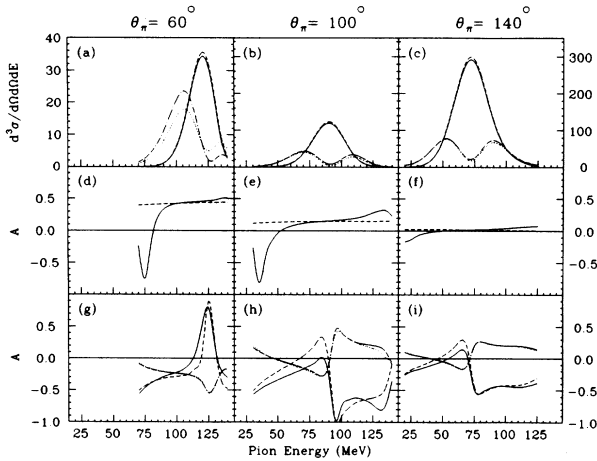


FIG. 5. Energy sharing cross sections and analyzing powers for the  $^{13}\text{C}(\pi^-, \pi^- n)^{12}\text{C}$  reaction at 165 MeV for the three angle pairs of Table II. Results are shown including (solid line) and omitting (dashed line) an emitted nucleon spin-orbit potential. The top graphs [(a)–(c)] show cross sections ( $\mu\text{b}/\text{sr}^2 \text{MeV}$ ) for  $1s_{1/2}$  and  $1p_{1/2}$  knockout. Graphs (d)–(f) are analyzing powers for  $1s_{1/2}$  knockout. Graphs (g)–(i) are analyzing powers for  $1p_{1/2}$  knockout to a  $0^+$  state and  $1p_{3/2}$  knockout to a  $2^+$  state. In the latter case the predictions with and without a spin-orbit potential are indicated by dotted and dot-dashed lines, respectively.

significant effects on the analyzing power (and even cross section) for the  $p_{1/2}$  knockout transition. These effects are large enough that it will be important to include the spin-orbit potential to obtain a good description of experimental analyzing powers. The differences between the effects on the  $p_{1/2}$  and  $p_{3/2}$  knockout analyzing powers presumably arise from the increased averaging over  $m$  states in the calculations for the  $j = \frac{3}{2}$  case.

#### B. DWIA calculations for $^{13}\text{C}(\pi^-, \pi^- n)^{12}\text{C}(J^\pi)$

For purposes of planning future experiments, DWIA calculations were carried out for the  $^{13}\text{C}(\pi^-, \pi^- n)^{12}\text{C}$  reaction at 165 MeV. The calculations use the parameters discussed previously, including the spin-orbit potential. The spectroscopic amplitudes were obtained using the wave functions of Cohen and Kurath.<sup>17</sup>

As previously noted, only for  $1^+$  final states do  $p_{1/2}$  and  $p_{3/2}$  terms interfere. As a result, the spectroscopic amplitudes reduce to the usual single nucleon spectroscopic factors for the remaining transitions.

Cross sections and analyzing powers for the three angle pairs listed in Table II are presented in Figs. 6–8. Figure 6 shows the results for the  $\frac{1}{2}^-$  to  $0^+$  ground-state transition. This transition is pure  $p_{1/2}$  knockout. The differences in shape compared with the previous calculations result primarily from  $Q$ -value effects.

In Fig. 7 are presented the results for the  $(1^+, T=0, 12.7 \text{ MeV})$  and  $(1^+, T=1, 15.1 \text{ MeV})$  states. Both transitions are, in fact, dominated by  $p_{3/2}$  knockout, hence the great similarity in analyzing powers. The cross sections, of course, differ. Note that, except for relatively small Coulomb differences, the  $(1^+, T=1)$  calculation is appropriate for the  $^{13}\text{C}(\pi^+, \pi^+ p)^{12}\text{N}(\text{g.s.})$  reaction.

Finally, in Fig. 8 we present the calculations for the  $(2^+, T=0, 4.4 \text{ MeV})$  and  $(2^+, T=1, 16.1 \text{ MeV})$  states. These are pure  $p_{3/2}$  transitions. The cross sections for the two states are comparable. Again, the differences in

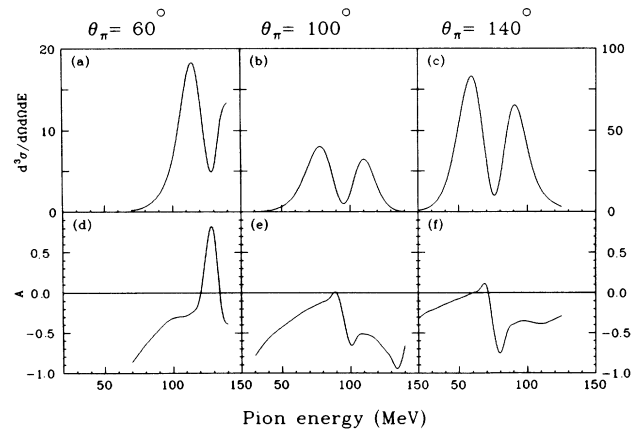


FIG. 6. Energy sharing cross sections ( $\mu\text{b}/\text{sr}^2 \text{MeV}$ ) and analyzing powers for  $^{13}\text{C}(\pi^-, \pi^- n)^{12}\text{C}(0^+, \text{ground state})$  reactions at 165 MeV for the single pairs of Table II. Graphs (b) and (c) use the right scale. Spectroscopic amplitudes are from Cohen and Kurath (Ref. 17).

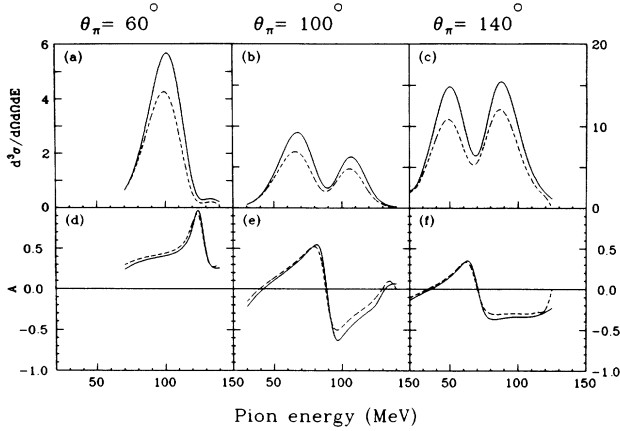


FIG. 7. Energy sharing cross sections ( $\mu\text{b}/\text{sr}^2\text{MeV}$ ) and analyzing powers for the  $^{13}\text{C}(\pi^-, \pi^-n)^{12}\text{C}$  reaction to the  $1^+$ ,  $T=0$ , 12.7 MeV state (solid line) and the  $1^+$ ,  $T=1$ , 15.1 MeV state (dashed line) at 165 MeV for the angle pairs of Table II. Graphs (b) and (c) use the right scale. Spectroscopic amplitudes are from Cohen and Kurath (Ref. 17).

analyzing powers are due to differences in  $Q$  value.

Based on previous comparisons between DWIA calculations and  $(\pi^+, \pi^+p)$  data, we expect that the present calculations will provide a reasonably good description of experimental data. They certainly are adequate in terms of designing and planning an experiment.

## V. SUMMARY AND CONCLUSIONS

Pion-induced nucleon knockout from polarized targets has been investigated in DWIA. The case of coplanar geometries and  $J_A = \frac{1}{2}$  targets has been considered with emphasis on light targets for which nucleons are ejected from  $1s$  and  $1p$  orbits. For the case of  $1p$  knockout, polarizing the target leads to an effective polarization in both orbital angular momentum and in spin for the struck nucleon. While these effects are clearly closely related it is, nevertheless, possible and useful to consider them independently. Thus, one can consider the reaction sensitive to the spin polarization through the pion-nucleon intrinsic polarization analyzing power leading to a term  $P_s A$ . Similarly, the orbital angular momentum polarization leads to a term  $P_0 P$ , which expresses any *preference* the reaction may have for different transferred orbital angular momentum projections. This can arise from localization effects, typically due to differences in mean free path for the two ejected particles. Finally, a third term arises,  $\alpha P A$ , in which, through the spin-orbit coupling, any *preference* in orbital angular momentum

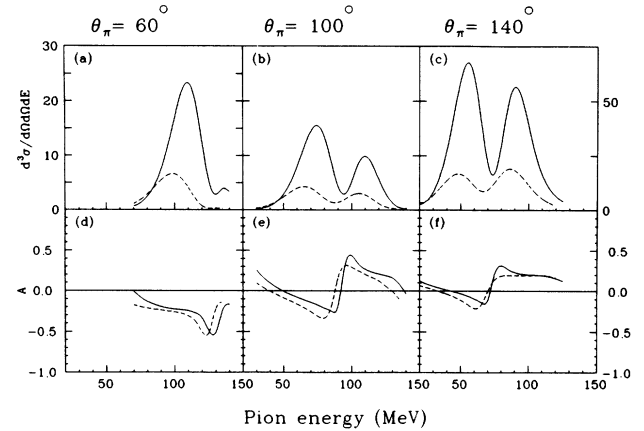


FIG. 8. Energy sharing cross sections ( $\mu\text{b}/\text{sr}^2\text{MeV}$ ) and analyzing powers for the  $^{13}\text{C}(\pi^-, \pi^-n)^{12}\text{C}$  reaction to the  $2^+$ ,  $T=0$ , 4.4 MeV state (solid line) and the  $2^+$ ,  $T=1$ , 16.1 MeV state (dashed line) at 165 MeV for the angle pairs of Table II. Graphs (b) and (c) use the right side. Spectroscopic amplitudes are from Cohen and Kurath (Ref. 17).

projection leads to a reaction *preference* in spin projection for the ejected nucleon. This last term is thus also sensitive to the intrinsic pion-nucleon polarization analyzing power. Since it is not a consequence of polarizing the target it does not lead to any target spin dependence (other than through an overall normalization of  $A_{\text{TGT}}$ ) and also survives in the case of an unpolarized target.

Sample DWIA calculations have confirmed the features outlined above and suggest that, for  $^{13}\text{C}(\pi^-, \pi^-n)^{12}\text{C}$  at 165 MeV, studies of the effective pion-nucleon polarization analyzing power are best done at forward angles of around  $\theta_\pi = 60^\circ$ . At larger pion angles of approximately  $\theta_\pi = 140^\circ$  values of  $A_{\text{TGT}}$  depend largely on dynamical effects such as mean free path differences.

Calculations including spin-orbit terms in the emitted nucleon optical potential suggest that it is important to include such terms, at least for  $p_{1/2}$  knockout.

Finally, fairly realistic predictions are made for the major transitions from  $^{13}\text{C}$  to  $^{12}\text{C}$  using the Cohen-Kurath wave functions. These should prove useful in designing  $^{13}\text{C}(\pi^-, \pi^-n)^{12}\text{C}$  experiments using a polarized  $^{13}\text{C}$  target.

## ACKNOWLEDGMENTS

We are indebted to our colleague G. Kyle for suggesting this problem. This work was supported in part by the National Science Foundation.

<sup>1</sup>P. B. Siegel and W. R. Gibbs, Phys. Rev. C **36**, 2473 (1987).

<sup>2</sup>G. Kyle, P.-A. Amaudruz, Th. S. Bauer, J. J. Domingo, C. H. Q. Ingram, J. Jansen, D. Renker, J. Zichy, R. Stamminger, and F. Vogler, Phys. Rev. Lett. **52**, 974 (1984).

<sup>3</sup>S. Gilad, S. Høibråten, W. J. Burger, G. W. Dodson, L. D. Pham, R. P. Redwine, E. Piasetzky, H. W. Baer, J. D. Bowman, F. H. Cverna, M. J. Leitch, U. Sennhauser, Th. S.

Bauer, C. H. Q. Ingram, G. S. Kyle, D. Ashery, S. A. Wood, and Z. Fraenkel, Phys. Rev. Lett. **57**, 2637 (1986).

<sup>4</sup>N. S. Chant, L. Rees, and P. G. Roos, Phys. Rev. Lett. **48**, 1784 (1982).

<sup>5</sup>M. Hirata, F. Lenz, and M. Thies, Phys. Rev. C **28**, 785 (1983).

<sup>6</sup>L. Rees, N. S. Chant, and P. G. Roos, Phys. Rev. C **26**, 1580 (1982).

- <sup>7</sup>P. G. Roos, L. Rees, and N. S. Chant, *Phys. Rev. C* **24**, 2647 (1981).
- <sup>8</sup>N. S. Chant and P. G. Roos, *Phys. Rev. C* **27**, 1060 (1983).
- <sup>9</sup>D. M. Brink and G. R. Satchler, *Angular Momentum* (Oxford University Press, New York, 1962).
- <sup>10</sup>H. C. Newns, *Proc. Phys. Soc. London, Sect. A* **66**, 477 (1953); H. C. Newns and M. Y. Refai, *ibid.* **71**, 627 (1958).
- <sup>11</sup>G. Jacob, Th. A. J. Maris, C. Schneider, and N. R. Teodoro, *Nucl. Phys.* **A257**, 517 (1976).
- <sup>12</sup>P. Kitching, C. A. Miller, W. C. Olsen, D. A. Hutcheon, W. J. McDonald, and A. W. Stetz, *Nucl. Phys.* **A340**, 423 (1980); L. Antonuk, P. Kitching, C. A. Miller, D. A. Hutcheon, W. J. McDonald, G. C. Neilson, W. C. Olsen, and A. W. Stetz, *ibid.* **A370**, 389 (1981).
- <sup>13</sup>W. B. Cottingham and D. B. Holtkamp, *Phys. Rev. Lett.* **45**, 1828 (1980).
- <sup>14</sup>J. F. Amann, P. D. Barnes, K. G. R. Doss, S. A. Dytman, R. A. Eisenstein, J. D. Sherman, and W. R. Wharton, *Phys. Rev. C* **23**, 1635 (1981).
- <sup>15</sup>A. Nadasen, P. Schwandt, P. P. Singh, W. W. Jacobs, A. D. Bacher, P. T. Debevec, M. D. Kaitchuck, and J. T. Meek, *Phys. Rev. C* **23**, 1023 (1981).
- <sup>16</sup>L. R. B. Elton and A. Swift, *Nucl. Phys.* **A94**, 52 (1967).
- <sup>17</sup>S. Cohen and D. Kurath, *Nucl. Phys.* **73**, 1 (1965); **A141**, 145 (1970).
- <sup>18</sup>P. Kitching, W. J. McDonald, Th. A. J. Maris, and C. A. Z. Vasconcellos, in *Advances in Nuclear Physics*, edited by J. W. Negele and E. Vogt (Plenum, New York, 1985), Vol. 15, p. 43.